Lecture 6: 2-D conservative systems and centers, closed orbits and limit-cycles, null-cline, heteroclinic orbit, the Dulac's criterion, the Poincaré-Bendixson theorem

Contents

Demonstration: Phase portrait of mathematical pendulum, periodic phase portrait of mathematical pendulum

1 Properties of conservative systems

We are continuing our analysis of conservative systems. In this section we introduce a theorem on centers and conservative systems.

1.1 Nonlinear centers in 2-D conservative systems

The theorem is presented on Slide 3. Figure 1 shows an **isolated fixed point** that has no other fixed points close to it.

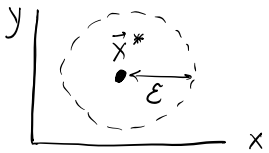

Figure 1: Isolated fixed point where $\varepsilon \ll 1$. No other fixed points exist inside the region shown with the dashed circle.

SLIDE: 3

Centers and conservative systems

Theorem: Suppose $\dot{\vec{x}} = \vec{f}(\vec{x})$ is conservative and $\vec{f}$ is continuously differentiable in $\vec{x} \in \mathbb{R}^2$. $E(\vec{x})$ is a conserved quantity and $\vec{x}^*$ is an **isolated fixed point**. If that fixed point is a local minimum or maximum of $E(\vec{x})$, then that isolated fixed point $\vec{x}^*$ is a **center**, i.e., all trajectories close to $\vec{x}^*$ are closed orbits.

D. Kartofelev YFX1520 3 / 23

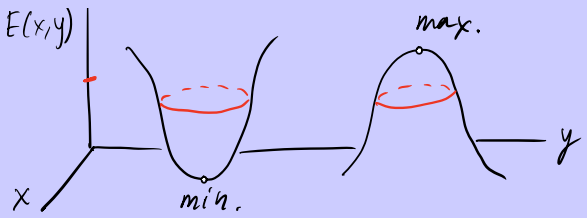

Figure 2: Closed trajectories close to the local minimum or maximum of conserved quantity $E(\vec{x})$. The closed orbits are shown with the red curves.

Theorem: Suppose $\dot{\vec{x}} = \vec{f}(\vec{x})$ is conservative and $\vec{f}$ is continuously differentiable in $\vec{x} \in \mathbb{R}^2$. $E(\vec{x})$ is a conserved quantity and $\vec{x}^*$ is an ***isolated fixed point*** shown in Fig. 1. If that fixed point is a local minimum or maximum of $E(\vec{x})$, as shown in Fig. 2, then that isolated fixed point $\vec{x}^*$ is a **center**, i.e., all trajectories close to $\vec{x}^*$ are closed orbits.

1.2 Example: Mathematical pendulum

1.2.1 Model and its fixed points

SLIDE: 4

Mathematical pendulum

Mathematical pendulum[1] is given in the following form:

$$\ddot{\theta} + \sin\theta = 0, \tag{1}$$

where θ is the angular displacement. For angular velocity $\omega = \dot{\theta}$ we rewrite the equation as follows

$$\begin{cases} \dot{\theta} = \omega, \\ \dot{\omega} = -\sin\theta. \end{cases} \tag{2}$$

[1] See Mathematica .nb file uploaded to the course webpage.

D. Kartofelev YFX1520 4 / 23

Figure 3: Mathematical pendulum where θ is the angular displacement.

The normalised and dimensionless model of mathematical pendulum is given by

$$\ddot{\theta} + \sin\theta = 0, \tag{1}$$

where θ is the angular displacement shown in Fig. 3. For angular velocity $\omega = \dot{\theta}$ we rewrite Eq. (1) as a system of first order ODEs

$$\begin{cases} \dot{\theta} = \omega, \\ \dot{\omega} = -\sin\theta. \end{cases} \tag{2}$$

Notice that Eq. (1) is explicitly independent of both $\dot{\theta}$ and t; hence there is no damping or friction of any kind, and there are no time-dependent external driving forces. This indicates that the system is conservative. Let's study the dynamics of pendulum model given by (1) for $-2\pi \leq \theta \leq 2\pi$. Fixed points (θ^*, ω^*) of the system are the following:

$$\ldots, (-2\pi, 0), (-\pi, 0), (0, 0), (\pi, 0), (2\pi, 0), \ldots \;\Rightarrow\; (\pm n\pi, 0), \quad \text{where } n \in \mathbb{Z}. \tag{3}$$

1.2.2 Proof of conserved quantity

We use Eq. (1) to prove the existence of a conserved quantity, which in this case is the total energy (see Lecture 5)

$$\ddot{\theta} + \sin\theta = 0 \quad | \cdot \dot{\theta},$$
$$\ddot{\theta}\dot{\theta} + \sin(\theta)\dot{\theta} = 0, \tag{4}$$

equivalently and for $\omega = \dot{\theta}$ we write

$$\frac{\mathrm{d}}{\mathrm{d}t}\left(\frac{\omega^2}{2} - \cos\theta\right) = 0, \tag{5}$$

where the first term corresponds to the kinetic energy and the second to the potential energy. The potential energy V follows directly from Eq. (1). How so? Since, force F is defined as

$$F = -\frac{\mathrm{d}V}{\mathrm{d}\theta}, \tag{6}$$

and since Eq. (1) is a balance of forces we derive the potential in the form

$$V = -\int(-\sin\theta)\mathrm{d}\theta = \int \sin\theta\,\mathrm{d}\theta = -\cos\theta + C, \tag{7}$$

where the integration constant $C = 0$. From (5) it is clear that the sum of the kinetic and potential energies is indeed conserved in time. Thus the conserved quantity/energy has the following form:

$$E(\theta,\omega) = \underbrace{\frac{\omega^2}{2}}_{\text{kin. en.}} \underbrace{-\cos\theta}_{\text{pot. en.}} = \text{const.} \tag{8}$$

Slide 5 shows the energy values as plotted against anglular displacement θ and angular velocity ω. The following numerical file contains the code that produced the plot.

NUMERICS: NB#1

Mathematical pendulum and heteroclinic orbit. Integrated numerical solution.

SLIDE: 5

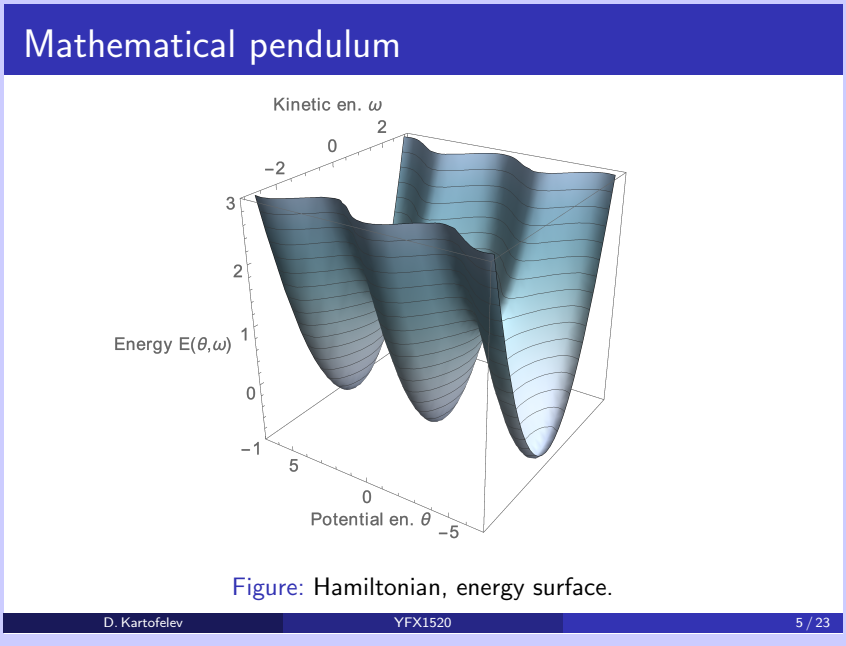

1.2.3 Linear analysis

Jacobian matrix of Sys. (2)

$$J = \begin{pmatrix} \dfrac{\partial\dot{\theta}}{\partial\theta} & \dfrac{\partial\dot{\theta}}{\partial\omega} \\ \dfrac{\partial\dot{\omega}}{\partial\theta} & \dfrac{\partial\dot{\omega}}{\partial\omega} \end{pmatrix} = \begin{pmatrix} 0 & 1 \\ -\cos\theta & 0 \end{pmatrix}. \tag{9}$$

Evaluation of the matrix about the selected system fixed points $(\theta^*, \omega^*) = (0,0)$, $(\pm\pi, 0)$, $(\pm 2\pi, 0)$ are the following:

$$J\big|_{(\theta^*,\omega^*)} = J\big|_{(0,0)} = J\big|_{(\pm 2\pi,0)} = \begin{pmatrix} 0 & 1 \\ -1 & 0 \end{pmatrix}, \tag{10}$$

here trace $\tau = 0$ and determinant $\Delta = 1$. According to the linear fixed point classification we have a **linear center** and according to the theorem presented in Sec. 1.1, this center is also a true **nonlinear center** because it is located at a local minimum of the *conserved quantity* (8), see Slide 5;

$$J\big|_{(\theta^*,\omega^*)} = J\big|_{(\pm\pi,0)} = \begin{pmatrix} 0 & 1 \\ 1 & 0 \end{pmatrix}, \tag{11}$$

here determinant $\Delta = -1$ and thus we have a **saddle**. Now we have all the information required to sketch the phase portrait shown on Slide 6.

The qualitatively accurate phase portrait and the interactive numerical solution of Eq. (1) or Sys. (2) are presented in the following numerical file.

NUMERICS: NB#1

Mathematical pendulum and heteroclinic orbit. Integrated numerical solution.

SLIDE: 6

Mathematical pendulum

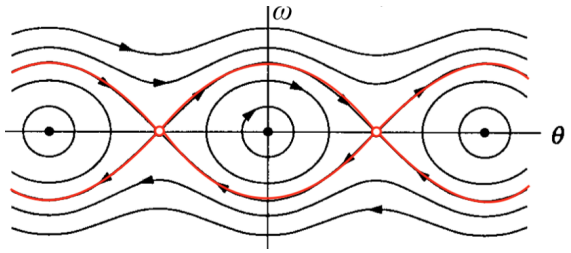

Figure: Phase portrait showing five fixed points $(\theta^*, \omega^*) = (-2\pi, 0)$, $(-\pi, 0)$, $(0,0)$, $(\pi, 0)$, $(2\pi, 0)$. Heteroclinic orbit is shown with the red curves.

D. Kartofelev YFX1520 6 / 23

We have encountered a new type of dynamics represented by the **heteroclinic** orbit. One could also argue that this orbit is **homoclinic** since the pendulum is 2π-periodic. Fixed points $(\pm 2\pi, 0)$ and $(0,0)$ or $(-\pi, 0)$ and $(\pi, 0)$ are actually the same fixed points.
Demonstration: Periodicity of fixed points on the $\omega\theta$-plane.

2 Limit-cycles

A **limit-cycle** is an *isolated closed trajectory*. Isolated means that neighbouring trajectories are not closed; they spiral either toward or away from the limit-cycle, see Fig. 4. If all neighbouring trajectories approach a limit-cycle, we say that this limit-cycle is **stable** or **attracting**. Otherwise the limit-cycle is **unstable** or **repelling**, or in exceptional cases, **half-stable**. Half-stable limit-cycle can be stable from inside and unstable from outside as shown in Fig. 4 (Right) or vice versa.

Stable limit-cycles are very important scientifically—they model systems that exhibit **self-sustained oscillations**. In other words, these systems oscillate even in the absence of external periodic forcing. Of the

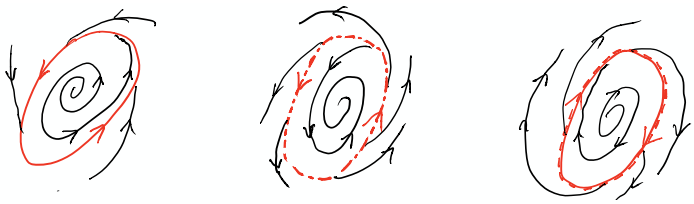

Figure 4: Limit-cycles are shown with the closed continuous or dashed red curves. Continuous curves indicate the stable and dashed the unstable limit-cycles. (Left) Stable or attracting limit-cycle. (Middle) Unstable or repelling limit-cycle. (Right) Half-stable limit-cycle that is stable from inside and unstable from outside.

countless examples that could be given, we mention only a few: the beating of a heart; the periodic firing of a pacemaker neurone; daily rhythms in human body temperature and hormone secretion; chemical reactions that oscillate spontaneously; and dangerous self-excited vibrations in bridges and airplane wings that can lead to structural damage and failure. In each case, there is a standard/nominal oscillation of some preferred period, waveform, and amplitude. If the system is perturbed slightly, it always returns to the nominal cycle. **Limit-cycles are inherently nonlinear phenomena** they can not occur in linear systems (by linear system we mean systems in a form: $\dot{\vec{x}} = A\vec{x}$, where system matrix A has constant and real valued coefficients).

3 Testing for closed orbits

3.1 The Dulac's criterion

The Dulac's criterion is a negative criterion used **to rule out limit-cycles**.

SLIDE: 7

The Dulac's criterion

Let $\dot{\vec{x}} = \vec{f}(\vec{x})$ be a continuously differentiable vector field defined on a *simply connected* subset R of a plane. If there exists a continuously differentiable, real valued function $g(\vec{x})$ such that

$$\mathrm{div}(g\dot{\vec{x}}) = \nabla \cdot (g\dot{\vec{x}}), \tag{3}$$

has one sign throughout R, then there are no closed orbits lying entirely in R.

Note: If the sign changes no conclusion can be made.

D. Kartofelev YFX1520 7 / 23

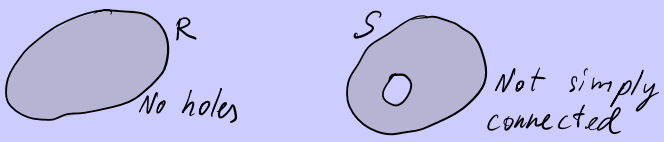

Figure 5: (Left) Simply connected region R having no *holes*. (Right) Not simply connected region S.

In a **simply connected** region it is possible to shrink the circumference or perimeter of the region to be infinitely small (not a technical definition). Figure 5 shows a comparison between a simply connected region and a not simply connected region.

3.1.1 Example 1

Show that system

$$\begin{cases} \dot{x} = x(2 - x - y), \\ \dot{y} = y(4x - x^2 - 3), \end{cases} \tag{12}$$

has no closed orbits in simply connected region R, where $x > 0$ and $y > 0$, shown in Fig. 6.

Figure 6: Region of interest in 2-D plain.

We have to come up with function $g(\vec{x})$. Based on an educated guess we pick the following function:

$$g = \frac{1}{xy}. \tag{13}$$

Now we need to study the sign of

$$\begin{aligned} \operatorname{div}(g\dot{\vec{x}}) = \nabla \cdot (g\dot{\vec{x}}) = \left(\frac{\partial}{\partial x}, \frac{\partial}{\partial y}\right) \cdot \begin{pmatrix} g\dot{x} \\ g\dot{y} \end{pmatrix} = \frac{\partial}{\partial x} g\dot{x} + \frac{\partial}{\partial y} g\dot{y} = \\ \frac{\partial}{\partial x}\left[\frac{x(2 - x - y)}{xy}\right] + \frac{\partial}{\partial y}\left[\frac{y(4x - x^2 - 3)}{xy}\right] = \\ \frac{\partial}{\partial x}\left(\frac{2 - x - y}{y}\right) + \frac{\partial}{\partial y}\left(\frac{4x - x^2 - 3)}{x}\right) = -\frac{1}{y} < 0. \end{aligned} \tag{14}$$

As can be seen the sign is negative in region R because $y > 0$. Since, the sign is strictly negative we do not have closed orbits in region R. We can confirm this conclusion using a computer. Numerical file linked below shows the phase portrait of Sys. (12).

NUMERICS: NB#2

The Dulac's criterion and limit-cycles. A numerical example: integrated solution and phase portrait.

Phase portrait of Sys. (12), shown below, confirms that there are no closed orbits in region R.

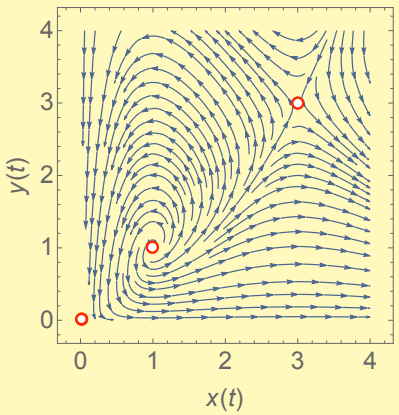

Figure 7: Phase portrait of Sys. (12) featuring three unstable fixed points shown with the empty bullets.

3.1.2 Example 2 *(home assignment)*

Show that system

$$\begin{cases} \dot{x} = y, \\ \dot{y} = -x - y + x^2 + y^2, \end{cases} \tag{15}$$

has no closed orbits in simply connected region $R \in \mathbb{R}^2$.

We have to come up with function $g(\vec{x})$. Based on an educated guess we pick the following function:

$$g = \mathrm{e}^{-2x}. \tag{16}$$

Now we need to study the sign of

$$\mathrm{div}(g\dot{\vec{x}}) = \nabla \cdot (g\dot{\vec{x}}) = \frac{\partial}{\partial x}\left(\mathrm{e}^{-2x} y\right) + \frac{\partial}{\partial y}\left[\mathrm{e}^{-2x}\left(-x - y + x^2 + y^2\right)\right] =$$
$$- \cancel{2\mathrm{e}^{-2x} y} - \mathrm{e}^{-2x} + \cancel{2\mathrm{e}^{-2x} y} = -\mathrm{e}^{-2x} < 0. \tag{17}$$

As can be seen the sign is negative in region R. Since, the sign is strictly negative we do not have closed orbits in the region $R \in \mathbb{R}^2$. We can confirm this conclusion using a computer. Numerical file linked below shows the phase portrait of Sys. (15).

NUMERICS: NB#3

The Dulac's criterion and limit-cycles. Numerical example: integrated solution and phase portrait.

Phase portrait of Sys. (15), shown below, confirms that there are no closed orbits in region $R \in \mathbb{R}^2$.

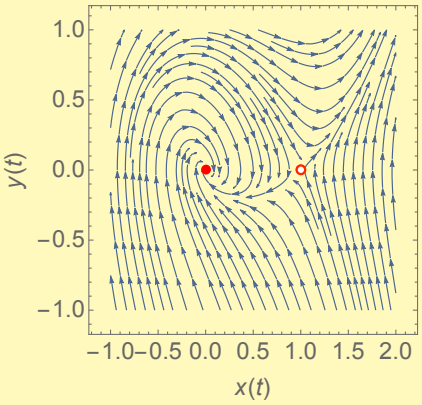

Figure 8: Phase portrait of Sys. (15) featuring stable spiral and unstable saddle node.

3.2 Proof of the Dulac's criterion

SLIDE: 10

Proof by contradiction, the Dulac's criterion

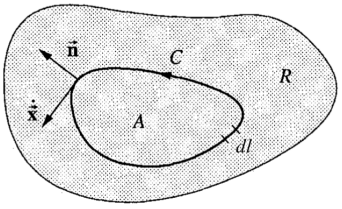

Let C be a closed orbit in subset R, and let A be the region inside C. Green's theorem:

$$\iint_A \left(\nabla \cdot \vec{F}\right) \mathrm{d}A = \oint_C \left(\vec{F} \cdot \vec{n}\right) \mathrm{d}l \tag{6}$$

If $\vec{F} = g\dot{\vec{x}}$, then

$$\iint_A \underbrace{\left[\nabla \cdot (g\dot{\vec{x}})\right]}_{\substack{\neq 0 \\ \text{has one} \\ \text{sign by} \\ \text{assumption}}} \mathrm{d}A = \oint_C \underbrace{\left(g\dot{\vec{x}} \cdot \vec{n}\right)}_{\substack{=0 \\ \vec{n} \perp \dot{\vec{x}}}} \mathrm{d}l \qquad \lightning \tag{7}$$

Therefore there is no closed orbit C in R.

D. Kartofelev YFX1520 10 / 23

Reminder: The dot product of two orthogonal vectors is 0.

3.3 The Poincaré-Bendixson theorem

Now that we know how to rule out closed orbits, we turn to the opposite task: finding a method to establish that closed orbits exist in particular systems. The following theorem is one of the few results in this direction.

SLIDE: 11

The Poincaré-Bendixson theorem

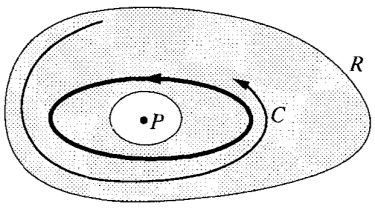

Suppose that:

1. R is a closed, bounded subset in $\mathbb{R}^2$, called the **trapping region**;
2. $\dot{\vec{x}} = \vec{f}(\vec{x})$ is a continuously differentiable vector field on an open set containing R;
3. R does not contain any fixed points (P); and
4. there exists a trajectory C that is "confined" in R, in the sense that it starts in R and stays in R for all future time.

Then either C is a closed orbit, or it spirals toward a closed orbit as $t \to \infty$. In either case, R contains a closed orbit (shown as a heavy closed curve in the above figure).

D. Kartofelev YFX1520 11 / 23

Trapping region R usually has an ***annular*** shape. Figure 9 shows a relatively *simple* trapping region. Trapping regions are not simply connected subsets of phase plane.

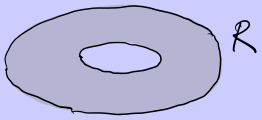

Figure 9: Trapping region R with annular donut-like shape.

Practical tip for constructing a trapping region: Select an annular region such that the vector field points/flows into it on its boundaries. According to the Poincaré-Bendixson theorem a closed orbit will be trapped in that annulus. Also, find and prefer annuli that have minimal area. Figure 10 shows an example of such annular region.

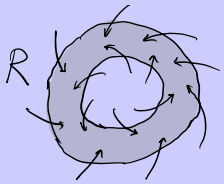

Figure 10: Annulus R with vector field vectors pointing into it on both of its boundaries.

3.3.1 Example 1

Consider the following system given in polar coordinates

$$\begin{cases} \dot{r} = r(1 - r^2) + \mu r \cos\theta, \\ \dot{\theta} = 1, \end{cases} \tag{18}$$

where μ is the control parameter. Show that closed orbits exist for small and positive μ, i.e., $0 < \mu \ll 1$.

For $\mu = 0$ the system takes the form

$$\begin{aligned} \dot{r} &= r(1 - r^2), \\ \dot{\theta} &= 1. \end{aligned} \tag{19}$$

This system is decoupled. Angular velocity $\dot{\theta}$ is constant and positive. The behaviour of a trajectory in the radial direction is described by the first equation. This equation is similar to the previously introduced logistic equation. 1-D phase portrait of the first equation is shown in Fig. 11. We can sketch the phase portrait corresponding to Sys. (19) by combining the above observations. Figure 12 shows the resulting phase portrait and the stable limit-cycle associated with the *carrying capacity* $r^* = K = 1$.

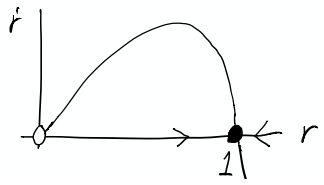

Figure 11: Phase portrait of the 1-D equation featured in (19) where the quantity similar the carrying capacity K of the logistic equation $r^* = K = 1$.

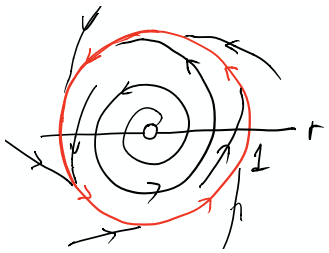

Figure 12: Phase portrait shown in polar coordinates corresponding to Sys. (19). Stable limit-cycle is shown with the red closed trajectory.

Let's consider the full system where $\mu \neq 0$ $(0 < \mu \ll 1)$. According to the Poincaré-Bendixson theorem we need to construct an annular trapping region. Figure 13 shows a promising candidate. We seek two concentric circles with radii $r = r_{\min}$ and $r = r_{\max}$ such that $\dot{r} < 0$ on the outer circle and $\dot{r} > 0$ on the inner circle. Then the annulus $0 < r_{\min} \leq r \leq r_{\max}$ will be our trapping region. Note that there are no fixed points in the annulus since $\dot{\theta} > 0 \neq 0$; hence, if $r_{\min}$ and $r_{\max}$ can be found, then the Poincaré-Bendixson theorem will imply the existence of a closed orbit.

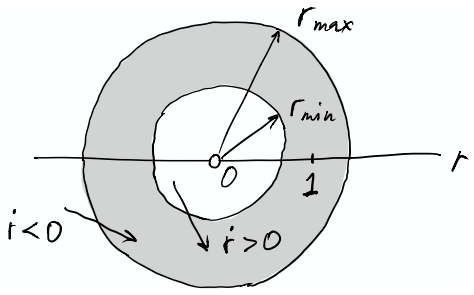

Figure 13: Annular trapping region shown in polar coordinates. The radial distance $r = r_{\min}$ is the inner boundary and $r = r_{\max}$ is the outer boundary of the proposed annulus.

Let's show that vector field defined by (18) flows into the selected annulus on its boundaries. Firstly, we consider the inner boundary $r = r_{\min}$ where it must hold that $\dot{r} > 0$ for all θ

$$\dot{r} = r(1 - r^2) + \mu r \cos\theta = r(1 - r^2 + \mu \cos\theta) > 0, \tag{20}$$

and since, $-1 \leq \cos\theta \leq 1$, a sufficient condition for $r_{\min}$ is

$$r(1 - r^2 - \mu) > 0 \quad | \div r, \tag{21}$$

$$1 - r^2 - \mu > 0, \tag{22}$$

$$r^2 < 1 - \mu, \tag{23}$$

$$r < \sqrt{1-\mu} \quad \Rightarrow \quad r_{\min} \lessapprox \sqrt{1-\mu}, \tag{24}$$

any such r will do as long as $\mu < 1$, which is fine since in our case $\mu \ll 1$.

Secondly, we consider the outer boundary $r = r_{\max}$ where it must hold that $\dot{r} < 0$ for all θ

$$\dot{r} = r(1 - r^2 + \mu\cos\theta) < 0, \tag{25}$$

and since once again, $-1 \leq \cos\theta \leq 1$, a sufficient condition for $r_{\max}$ is

$$r(1 - r^2 + \mu) < 0 \quad | \div r, \tag{26}$$

$$1 - r^2 + \mu < 0, \tag{27}$$

$$r^2 > 1 + \mu, \tag{28}$$

$$r > \sqrt{1+\mu} \quad \Rightarrow \quad r_{\max} \gtrapprox \sqrt{1+\mu}. \tag{29}$$

Now that $r_{\min}$ and $r_{\max}$ have been found we have proven the existence of a limit-cycle. Obtained result can be confirmed using a computer.

NUMERICS: NB#4

The Poincaré-Bendixson theorem. Phase portrait of a nonlinear system given in polar coordinates.

Numerically obtained results agree with the math derived above.

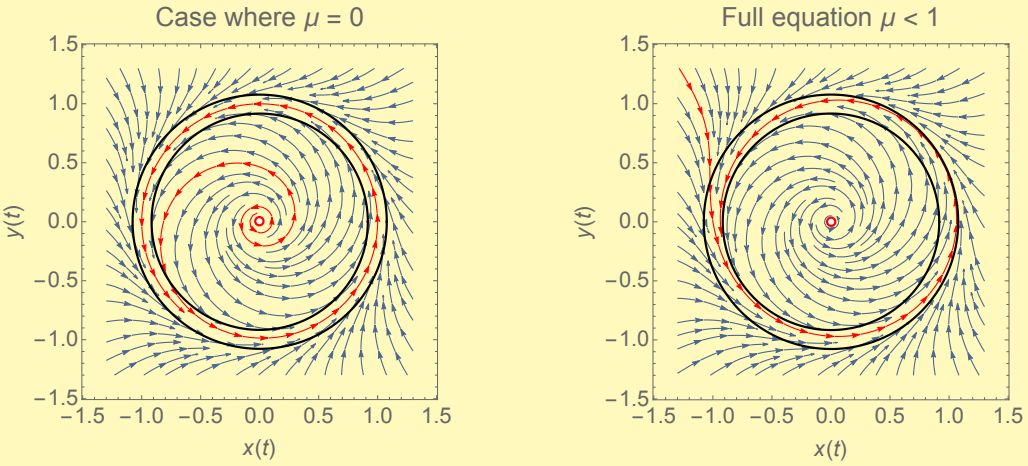

Figure 14: Phase portraits of Sys. (18) featuring a stable limit-cycle shown with the closed red trajectory. Annular trapping region is shown with the black concentric circles.

Note: The limit-cycle will also persist for $\mu > 1$, *cf.* (24).

3.3.2 Example 2: Glycolysis

This example is less contrived compared to the previous one. Let's consider a simplified dimensionless model of glycolysis given by

$$\begin{cases} \dot{x} = -x + ay + x^2 y, \\ \dot{y} = b - ay - x^2 y, \end{cases} \tag{30}$$

where a and b are the kinetic parameters, x and y are the concentrations of adenosine diphosphate (ADP) and fructose-6-phosphate (F6P) molecules, respectively. Here, $x, y, a, b > 0$.

Our tasks are:

1. Using the Poincaré-Bendixson theorem show that chemical oscillations are possible.
2. Determine the values of a and b that lead to the oscillating chemical reaction.

3.3.3 Null-clines

A useful tools for studying phase portraits are **null-clines**. The null-clines are curves on the 2-D phase portrait corresponding to $\dot{x} = 0$ and $\dot{y} = 0$. In the case $\dot{x} = 0$ and for the first equation in Sys. (30) we write

$$\dot{x} = 0 \quad \Rightarrow \quad -x + ay + x^2 y = 0 \quad \Rightarrow \quad y_{\dot{x}=0}(x) = \frac{x}{a + x^2}. \tag{31}$$

In the case $\dot{y} = 0$ and for the second equation in Sys. (30) we write

$$\dot{y} = 0 \quad \Rightarrow \quad b - ay - x^2 y = 0 \quad \Rightarrow \quad y_{\dot{y}=0}(x) = \frac{b}{a + x^2}. \tag{32}$$

The point where null-clines intersect each other corresponds to a fixed point. Null-clines (31) and (32) are sketched by hand in Fig. 15, along with some representative flow vectors. An easy way to determine the flow direction of the vector field defined by Sys. (30) is to estimate or calculate one vector and deduce the others by relying on the fact that the field must be continuous. We estimate that for $x \gg 1$ vector components $\dot{x} \approx x^2 y > 0$ and $\dot{y} \approx -x^2 y < 0$, notice that the terms $x^2 y$ and $-x^2 y$ are the most dominant terms in their respective equations. This vector, shown in the upper-right corner of Fig. 15, is used as a starting point to populate the phase portrait with the other vectors.

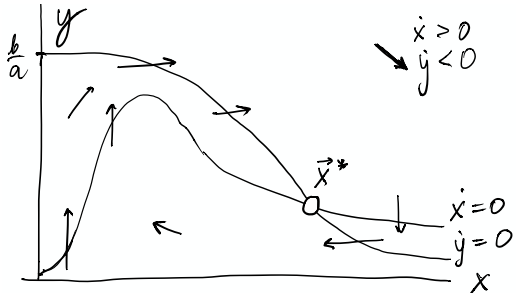

Figure 15: Null-clines (31) and (32). Flow direction of the vector field is shown with the arrows. Fixed point $\vec{x}^* = (x^*, y^*)^T$ shown with the hollow bullet is assumed to be unstable.

Slide 14 shows a promising trapping region. If we can show that vector field defined by Sys. (30) flows into this trapping region, then we have proven the existence of a closed orbit.

SLIDE: 14

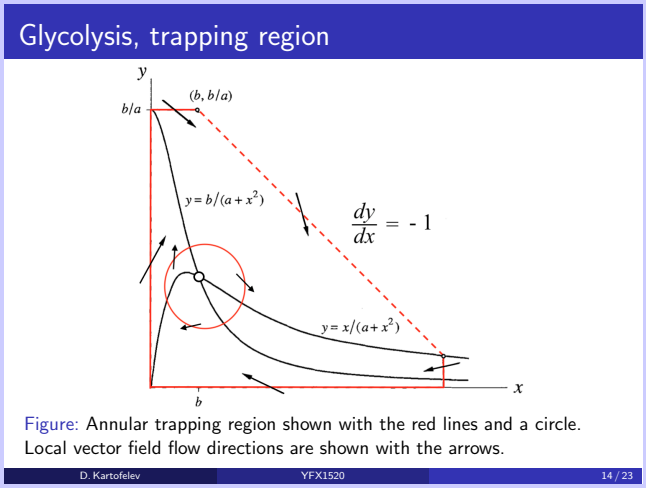

Null-clines (31) and (32) are shown with the continuous black curves.

First, we focus on the outer boundary. It is evident that the flow direction on the outer boundaries shown with the continuous red lines on Slide 14 is indeed pointing into the annulus. But, it is not so clear with the upper-right slanted part of the boundary shown with the dashed red line—How was point $x = b$ selected and why the slope $\mathrm{d}y/\mathrm{d}x = -1$ was selected?

As shown above the slope of the field vectors for $x \gg 1$ can be easily approximated from the algebraically dominant parts of field (30) $\dot{x} \approx x^2 y$ and $\dot{y} \approx -x^2 y$. The slope $\mathrm{d}y/\mathrm{d}x = \dot{y}/\dot{x} \approx -1$. This approach does not seem accurate enough in this application. We should compare the sizes of $\dot{x}$ and $-\dot{y}$ more precisely. The difference

$$\dot{x} - (-\dot{y}), \tag{33}$$

is

$$-x + \cancel{ay} + \cancel{x^2 y} + (b - \cancel{ay} - \cancel{x^2 y}), \tag{34}$$

$$b - x. \tag{35}$$

Thus the aforementioned difference is exactly zero for $x = b$ and

$$-\dot{y} > \dot{x}, \quad \text{for } x > b. \tag{36}$$

This inequality implies that the vector field points inward on the slanted outer boundary line shown on Slide 14, because $\mathrm{d}y/\mathrm{d}x$ is more negative than -1, and therefore the vectors are steeper than the boundary. Also, the question regarding the selection of point $x = b$ is answered here.

Now let's focus on the vector field flow through the inner boundary of the trapping region.

SLIDES: 15–19

Glycolysis, inner boundary of the trapping region

Secondly, we focus on the inner boundary of the proposed trapping region. We need to find and show that the fixed point

$$\begin{cases} \dot{x} = 0 \\ \dot{y} = 0 \end{cases} \Rightarrow \begin{cases} -x^* + ay^* + x^{*2}y^* = 0 \\ b - ay^* - x^{*2}y^* = 0 \end{cases} \Rightarrow (x^*, y^*) = \left(b, \frac{b}{a + b^2}\right), \tag{10}$$

is unstable, i.e., it repels the local vector field.

D. Kartofelev YFX1520 15 / 23

Glycolysis, inner boundary of the trapping region

We analyse fixed point (10) using linear analysis. The Jacobian of Sys. (9) has the following form:

$$J = \begin{pmatrix} \frac{\partial \dot{x}}{\partial x} & \frac{\partial \dot{x}}{\partial y} \\ \frac{\partial \dot{y}}{\partial x} & \frac{\partial \dot{y}}{\partial y} \end{pmatrix} = \begin{pmatrix} 2xy - 1 & a + x^2 \\ -2xy & -a - x^2 \end{pmatrix}. \tag{11}$$

D. Kartofelev YFX1520 16 / 23

Glycolysis, inner boundary of the trapping region

The Jacobian evaluated at fixed point (10) takes the form

$$J|_{(x^*, y^*)} = \begin{pmatrix} \frac{2b^2}{a + b^2} - 1 & a + b^2 \\ -\frac{2b^2}{a + b^2} & -a - b^2 \end{pmatrix}. \tag{12}$$

It's determinant $\Delta = \det J|_{(x^*, y^*)} = a + b^2 > 0$ is positive because $a, b > 0$, and its trace

$$\tau = \operatorname{tr} J|_{(x^*, y^*)} = \frac{2b^2}{a + b^2} - 1 - a - b^2. \tag{13}$$

D. Kartofelev YFX1520 17 / 23

Glycolysis, inner boundary of the trapping region

In order to ensure repelling unstable fixed points for $\Delta > 0$ trace τ has to be positive. The dividing line between repelling unstable fixed points and stable ones is $\tau = 0$. Solving

$$\tau = 0 \quad \Rightarrow \quad \frac{2b^2}{a + b^2} - 1 - a - b^2 = 0, \tag{14}$$

for b gives

$$b(a) = \sqrt{\frac{1}{2}\left(1 - 2a \pm \sqrt{1 - 8a}\right)}. \tag{15}$$

This result defines a line in the parameter space of Sys. (9). For parameters a and b in the region corresponding to $\tau > 0$, we are guaranteed that Sys. (9) has a closed orbit—an oscillating chemical reaction.

D. Kartofelev YFX1520 18 / 23

In order to ensure repelling unstable fixed points for $\Delta > 0$ trace τ has to be positive. Figure 16 shows the positions of repelling fixed points as they appear on the classification graph for the linear fixed points. The result shown on Slide 18 defines a curve in the parameter space of Sys. (30) shown on

Slide 19. For parameters a and b in the region corresponding to $\tau > 0$, we are guaranteed that Sys. (30) has a closed orbit—a self-sustained oscillating chemical reaction.

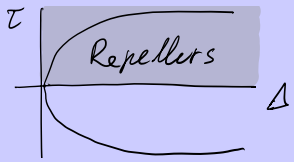

Figure 16: The Δ vs. τ fixed point classification graph. The marked region is populated by **repellers**: unstable nodes, unstable spirals, unstable stars, and unstable degenerate nodes.

Glycolysis, inner boundary of the trapping region

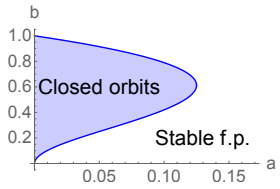

Figure: Parameter space defining the parameter values corresponding to unstable fixed point given by (10).

D. Kartofelev YFX1520 19 / 23

The result shown on Slide 19 was calculated using the following numerical file.

NUMERICS: NB#5

Glycolysis phase portrait and null-clines. Numerical solution of the glycolysis model.

We conclude that the annulus shown on Slide 14 is indeed the trapping region and a closed orbit exists in it. Numerical integration shows that closed orbit is a stable limit-cycle. Slides 20 and 21 show the phase portrait and numerically integrated time-domain results for a typical case where $a = 0.07$, $b = 0.53$.

SLIDES: 20, 21

Glycolysis[3], limit-cycle

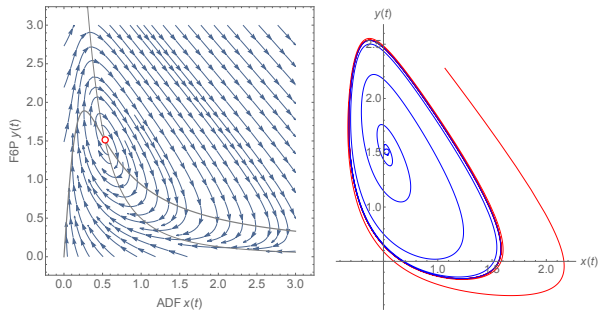

[3]See Mathematica .nb file uploaded to the course webpage.

D. Kartofelev YFX1520 20 / 23

Glycolysis, time-domain results

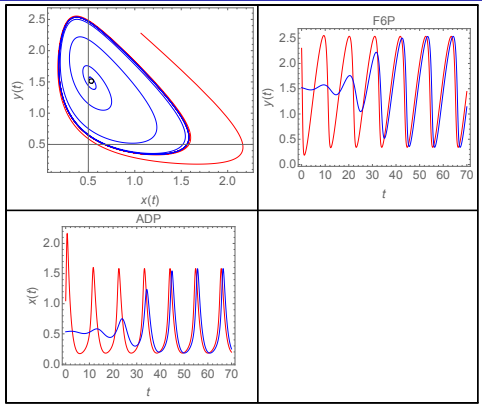

D. Kartofelev YFX1520 21 / 23

Numerical file that was used to generate the above figures is shown below.

NUMERICS: NB#5

Glycolysis phase portrait and null-clines. Numerical solution of the glycolysis model.

Phase portrait and null-clines for a typical case where $a = 0.07$, $b = 0.53$.

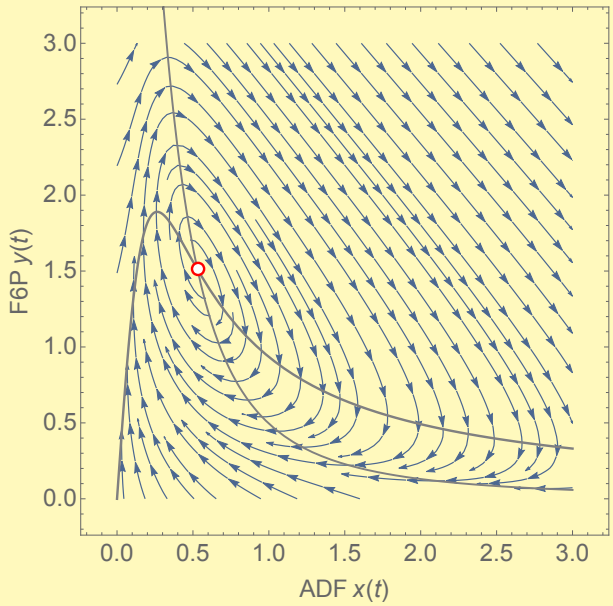

Figure 17: Phase portrait and null-clines of Sys. (30).

3.4 Implications of the Poincaré-Bendixson theorem

The Poincaré-Bendixson theorem is one of the central results of nonlinear dynamics. It says that the dynamical possibilities in the phase plane are very limited: if a trajectory is confined to a closed, bounded region that contains no fixed points, then the trajectory must eventually approach a closed orbit. Nothing more complicated is possible. This result depends crucially on the two-dimensionality of the plane. In higher-dimensional systems ($n \geq 3$), the Poincaré-Bendixson theorem no longer applies. The theorem also implies that *chaos* can never occur in the phase plane. The chaotic dynamics will be explained in future lectures.

Reading suggestion

Link	File name	Citation
Paper#1	paper0.pdf	Evgeni E. Sel'kov, "Self-oscillations in glycolysis 1. A simple kinetic model," *European Journal of Biochemistry*, **4**(1), pp. 79–86, (1968) doi:10.1111/j.1432-1033.1968.tb00175.x

Revision questions

1. Expand on the connection between 2-D conservative systems and centers.
2. Sketch a heteroclinic orbit.
3. What is limit-cycle?
4. Sketch a stable limit-cycle.
5. Sketch an unstable limit-cycle.
6. Sketch a half-stable (stable from outside) limit-cycle.
7. Sketch a half-stable (stable from inside) limit-cycle.
8. Define and sketch a null-cline.
9. What is the Dulac's criterion?
10. State the Poincaré-Bendixson theorem.
11. Does the Poincaré-Bendixson theorem apply to 3-D systems?
12. Can chaos occur in 2-D systems?